Liyan Liu
School of Chemical Engineering and Technology, Tianjin University, 135 Yaguan Road, Haihe Educational Park, Tianjin 300354, China
e-mail: liuliyan@tju.edu.cn

Jiaxiang Feng
School of Chemical Engineering and Technology, Tianjin University, 135 Yaguan Road, Haihe Educational Park, Tianjin 300354, China
e-mail: fjx_tju@163.com

Hao Wu
School of Chemical Engineering and Technology, Tianjin University, 135 Yaguan Road, Haihe Educational Park, Tianjin 300354, China
e-mail: wwwhha@126.com

Wei Xu
School of Chemical Engineering and Technology, Tianjin University, 135 Yaguan Road, Haihe Educational Park, Tianjin 300354, China
e-mail: xw1224@tju.edu.cn

Wei Tan[1]
School of Chemical Engineering and Technology, Tianjin University, 135 Yaguan Road, Haihe Educational Park, Tianjin 300354, China
e-mail: wtan@tju.edu.cn

Fluid Excitation Forces on a Tightly Packed Tube Bundle Subjected in Cross-Flow

Fluid excitation forces acting on stationary cylinders with cross-flow are the coupling of vortex shedding and turbulence buffeting. Those forces are significant in the analytical framework of fluid-induced vibration in heat exchangers. A bench-scale experimental setup with an instrumented test bundle is constructed to measure fluid excitation forces acting on cylinders in the normal triangular tube arrays ($P/D = 1.28$) with water cross-flow. The lift and drag forces on stationary cylinders are measured directly as a function of Reynolds number with a developed piezoelectric transducer. The results show that the properties of fluid excitation forces, to a great extent, largely depend upon the locations of cylinders within bundle by comparison to the inflow variation. A quasi-periodic mathematical model of fluid excitation forces acting on a circular cylinder is presented for a tightly packed tube bundle subjected to cross-flow, and the bounded noise theory is applied between $f_R = 0.01$ and $f_R = 1$. The developed model is illustrated with lots of identification results based on the dominant frequency, the intensity of random frequency, and the amplitude of fluid excitation forces. A second model has been developed for fluid excitation forces between $f_R = 1$ and $f_R = 6$ with the spectrum index introduced. Although still preliminary, each model can predict the corresponding forces relatively well.
[DOI: 10.1115/1.4035318]

1 Introduction

Flow-induced vibration of tube arrays is one of the important reasons for the long-term fretting-wear or fatigue within the steam generators and other heat exchangers. Generally, the mechanisms for flow-induced vibration consist of vortex shedding, turbulence buffeting, and fluid-elastic instability [1]. The structural vibration, generated by alternating shedding of vortices, is strongly nonlinear structural response with multifrequencies [2]. The turbulence buffeting can cause comparatively small-amplitude vibrations under normal conditions among these mechanisms. However, it finally induces the progressive damage of tubes [3].

In practical cases, the flow-induced vibration problems are too complicated to distinguish from these mechanisms which can scarcely exist independently. They can lead to the complex dynamic behavior of the cross-flow-induced excitation forces and the fluid–structure system [4]. According to Naudascher and Rockwell [5], the total cross-flow-induced excitation force, F_{total}, can be expressed as

$$F_{\text{total}} = F_M + F_V + F_T \tag{1}$$

where F_M, F_V, and F_T represent the motion-dependent, vortex-induced, and turbulence-induced buffeting force, respectively. If the cylinders are rigid and fixed, their behavior can become stationary with cross-flow. Under these circumstances, the total cross-flow-induced excitation force, F_{total}, can be expressed as

$$F_{\text{total}} = F_{V0} + F_{T0} \tag{2}$$

where F_{V0} and F_{T0} represent the vortex-induced force and the turbulence-induced buffeting force without tube motion. Three theories are applied in the motion-dependent fluid force: quasi-static flow theory, in which the fluid excitation forces acting on cylinders are attributed to variations in the tube position only [6];

[1]Corresponding author.

Contributed by the Pressure Vessel and Piping Division of ASME for publication in the Journal of Pressure Vessel Technology. Manuscript received August 26, 2016; final manuscript received November 1, 2016; published online January 11, 2017. Assoc. Editor: Tomomichi Nakamura.

quasi-steady flow theory, in which fluid excitation forces acting on cylinders are attributed to variations in tube velocity in addition to the tube position [7]; and unsteady flow theory, in which the unsteady fluid excitation forces acting on cylinders have a high similar characteristics to those acting on cylinders which are performing periodic oscillations [8]. In fact, no matter what theory the motion-dependent fluid forces are based on, all of them are dependent upon deviation from the reference state of steady flow [9]. The coefficients of the motion-dependent fluid forces are associated with lots of system parameters. In the quasi-static and quasi-steady flow theories, the fluid-force coefficients are mainly dependent of the arrangement, considering the tube velocity is much smaller than the flow velocity. Thorsen et al. [10] predict the observed hydrodynamic damping for cross-flow in stationary incoming flow with an advanced model. They simulate the vortex-induced vibration of an elastic cylinder in oscillating flow. For a stationary cylinder, the vortex-induced force is also stationary and can be represented by the bounded noise processes [11]. When the flow velocity is dominant compared with the velocity of cylinder vibration, the unsteady vortex-induced force is equivalent to it acting on a similar stationary cylinder, but with the direction of the flow approach changed by the velocity of cylinder vibration. Meanwhile, Zhu et al. [12] develops the model of grid-generated turbulence based on the bounded noise processes hypothesis.

Fluid excitation forces and the relationships between vortex shedding and turbulence buffeting have been extensively measured and analyzed. The fluid excitation forces are connected with the locations of the cylinders and the conditions of the incoming flow [13]. The influence of the upstream flow is very significant for both periodic and stochastic components. The fluctuating vortex-induced forces for various tube arrays are presented by Pettigrew and Ko [14], and some of the forces are deduced from tube responses, not from direct force measurement. Once the fluid has passed the first few rows, fluid excitation forces are not sensitive to the locations of cylinders any more [15]. The drag and lift forces obtained by Heinecke and Mohr [16] for square arrays in a range of Reynolds numbers show that the unsteady lift force is almost independent of Reynolds number.

Compared with the current mainstream approach about fluid forces, the quasi-periodic model, which tries to integrate the coupling effects of periodic and stochastic components of fluid forces, is much more worthy of attention. Especially, the vortex shedding is always simplified and ignored in the current turbulence model [17]. The influences of turbulence buffeting on vortex shedding have been proven by the experimental results with the fluid force measurement and flow rate measurement [18,19]. The formation of vortex shedding is obviously affected by turbulence buffeting, and the similar phenomenon has been founded in the study of two-phase flow [20]. Unfortunately, there is no suitable quasi-periodic fluid forces model published in the present studies.

This work aims at understanding the nature of the unexpected quasi-periodic fluid excitation forces originated by vortex shedding and turbulence buffeting. An experiment program was undertaken to measure the motion-independent fluid excitation forces acting on cylinders in the normal triangular tube arrays subjected to cross-flow. Both of lift force and drag force were measured directly with a piezoelectric transducer installed on the cylinders. Based on the theories of the bounded noise and the spectrum index, experimental expression models for power spectral density (PSD) of the motion-independent fluid excitation forces were proposed.

2 Experimental Setup

For fluid forces' measure, researchers have investigated horizontal tube bundle by experimental setup with bisupport, which need double force transducers working synchronously and horizontal flexible seals such as a rubber tub. Thus, complete synchronization and additional external interference idealization are required in their experiments. Compared with them, this work is without that specific requirement. A schematic of the experimental facility is shown in Fig. 1. The experiment was conducted in a circulating water channel with an essentially rectangular cross section (160 mm × 166 mm), which was 3000 mm long to ensure the inflow steady. The test-section consisted of five rows of cylinders, normal triangular tube arrays with a pitch to diameter ratio of 1.28 to simulate essentially the flow path in a tightly packed tube bundle with water cross-flow.

The cylinders were made of aluminum and had qualitatively similar surface roughness. All tubes in the test-section shared the same height through the thread adjustment in addition to the test cylinders, with a length of $l = 300$ mm including the caring zone ($l = 155$ mm). The upper end of the test cylinder was fixed on a support with sensor connection. The dynamic lift and drag forces were measured, using the force measuring device, as shown in Fig. 2. For tubes, the nature frequency ($f_1 = 533.751$ Hz) and Scruton number (Sc = 72.200) are required to be big enough. The force transducer was fixed to a rigid frame outside the test section to eliminate transmission of vibration to the transducer with a fixed support. Since tubes' resonance frequency must be sufficiently higher than the maximum frequency of interest to avoid the interference, a stiff system with fixed structure of cantilever beam was applied. In this way, the fluctuating forces on the cylinder were directly sensed by TYPE LC1330 transducer at the upper end of the cylinder. The data acquisition system, model DH5922, was used to sample rate of 1000 samples per second, as shown in Fig. 3.

Tube arrangement is shown in Fig. 4. Different tubes are denoted by symbols of 1, 2, 3, 4, and 5, considering the fluid dynamic forces acting on tubes in different positions. For ease of

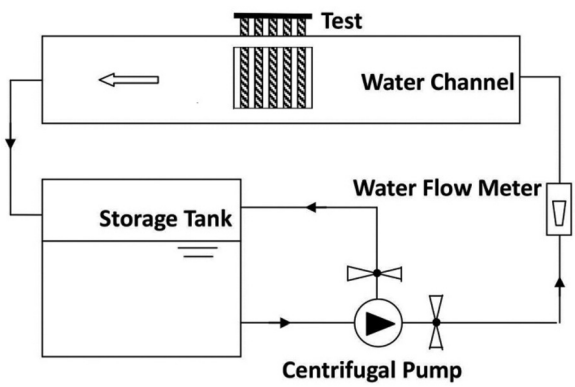

Fig. 1 Schematic of the experimental set

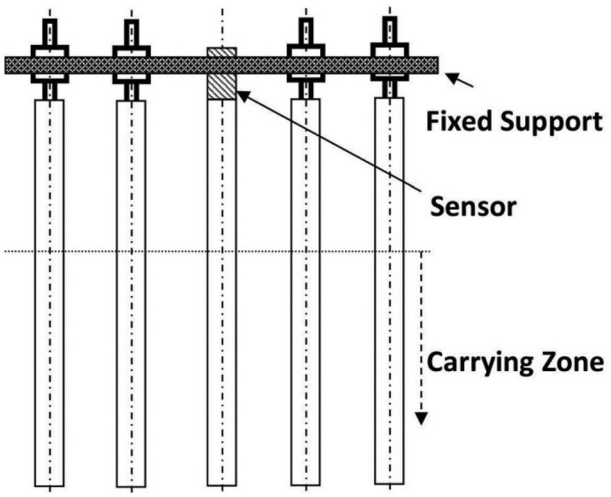

Fig. 2 Schematic of the test-section

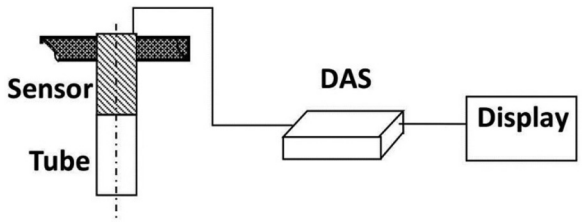

Fig. 3 Schematic of DAS

comparison, the Reynolds number is calculated using the gap velocity, V_P, which is given by

$$V_P = V_0 \times \frac{P}{P-D} \tag{3}$$

where V_0 is the free stream velocity. The tests were done over a wide range of Reynolds numbers, from 1.79×10^4 to 5.38×10^4.

3 Test Results

3.1 Vortex Shedding. In fact, the research about vortex shedding has already been studied deeply. In this work, the results can be used as the basic prop theory of the random turbulence model. Fluid excitation forces induced by vortex shedding are essentially periodic exciting force, characterized by specific frequencies and amplitudes. For tube arrays, the reduced frequency, f_R, can be expressed as

$$f_R = \frac{f_v D}{V_P} \tag{4}$$

where f_v is the vortex shedding frequency. The reduced frequency of fluctuating lift force is equivalent to Strouhal number, St. When the vortex-induced shedding force is not discrete any more, the coefficients of fluctuating drag and lift forces are defined by the root mean square value of the drag and lift forces, C_l and C_d expressed as

$$C_l = \frac{F_{l\,\mathrm{rms}}}{\frac{1}{2}\rho D L V_P^2} \tag{5}$$

$$C_d = \frac{F_{d\,\mathrm{rms}}}{\frac{1}{2}\rho D L V_P^2} \tag{6}$$

Figure 5 shows the fluctuating lift and drag forces from tube 1 to tube 5 at $\mathrm{Re} = 3.07 \times 10^4$. With flow passing through the staggered array, fluctuating fluid forces change from highly organized to random, and the overall amplitude of fluctuating fluid forces increases gradually. The organized property of fluctuating fluid forces is indicative of the orderly alternate vortex shedding. Highly nonuniform flow or rambling turbulence causes the global characteristics converted. The phase differences of fluid forces for the first three rows are shown in Fig. 6. The phase difference on the early stage of fluid disturbance (the upstream rows) when the fluid is quite organized is hard to figure out because of the interference of turbulence. There is no observable interaction of tube layout.

The characteristic parameters of the vortex-induced shedding force for five rows of tubes in the lift and drag direction are shown in Figs. 7 and 8. With the increase of Reynolds number, the lift force coefficient, C_l, decreases slightly, while there is no significant change of the reduced frequency, fD/V_P. The fluid forces for downstream tube are insensitive to the incoming flow conditions, because of the progress of the measured fluid force coefficient as a function of the row. For the interior tubes (tubes beyond the third row), the values of these coefficients become small and approximately keep constant. The turbulence-induced buffeting force has played a dominant role in fluid forces. The drag force coefficient, C_d, is smaller than C_l because of alternate shedding vortex leading to the dynamic pressure difference between both sides of the cylinder. Even based on the available experimental data of the lift force, St for each tube cannot be precisely determined. Among the downstream tubes, the periodic vortex shedding has no distinct frequency, replaced by the stochastic noise. Part of the results is estimated based on the main peak above all the others.

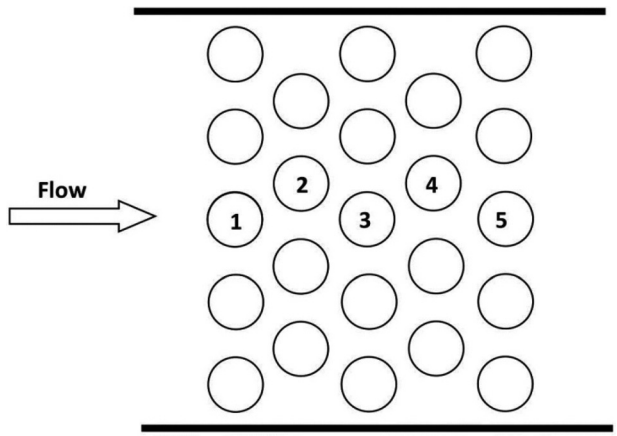

Fig. 4 Tube arrangement

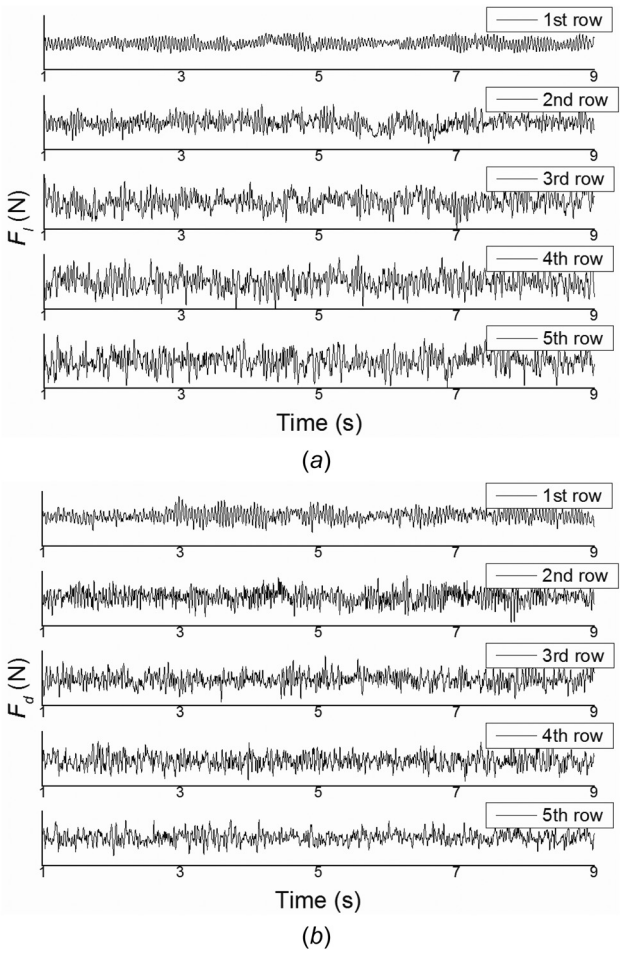

Fig. 5 Fluctuating lift and drag forces

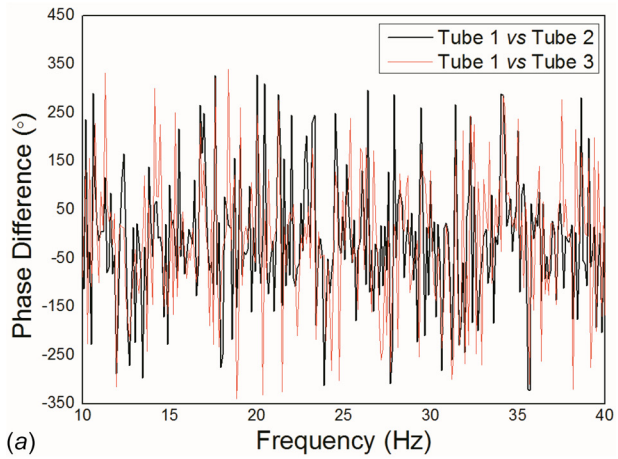

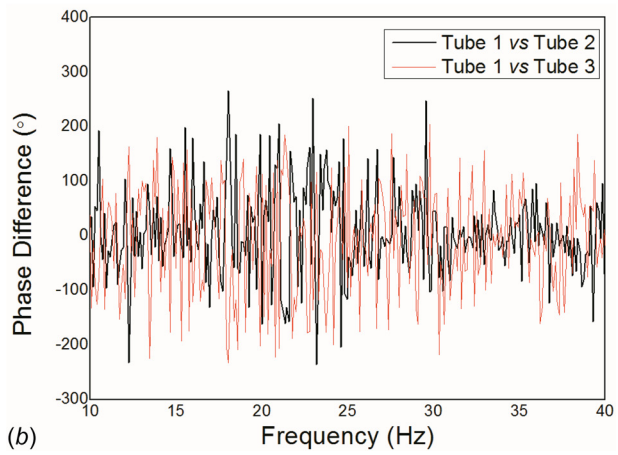

Fig. 6 Phase difference of fluid forces

3.2 Turbulence Buffeting. The function of turbulence-induced buffeting force is determined by model testing, dimensional analysis, and probabilistic structure dynamic analysis with a hybrid experimental/analytical integral approach. The mean square of tube response for model 1, the final form applied to cross flow in tube arrays, can be expressed as follows [21]:

$$\overline{y^2(x)_1} = \frac{\phi_1^2(x) S_F(f) J_1^2}{64\pi^3 f_1^3 M_1^2 \zeta_1} \tag{7}$$

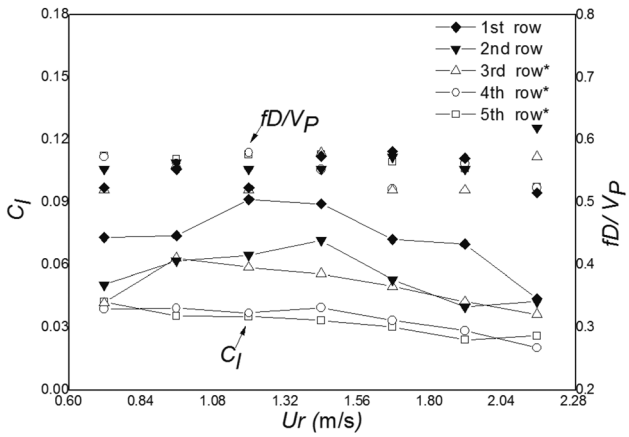

Fig. 7 Characteristic parameters of the fluctuating lift force

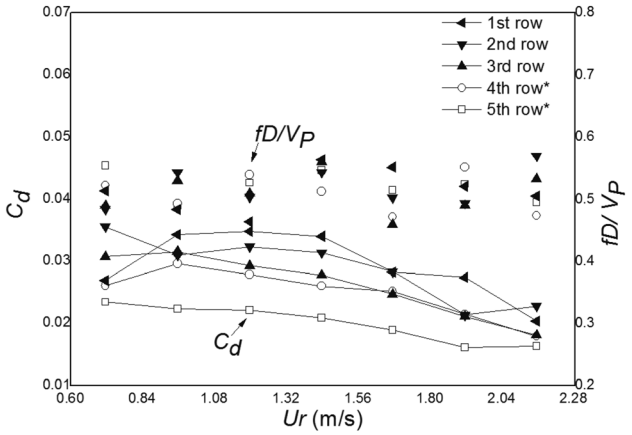

Fig. 8 Characteristic parameters of the fluctuating drag force

where $S_F(f)$ is the auto-power spectral density of the input force per unit length. The joint acceptance, J_1^2, can be calculated if the correlation length, λ, is known. The data are lacking over a tightly packed tube bundle, and the correlation length, λ, can be expressed as follows [22]:

$$\lambda \approx 0.2P\left(1 + \frac{P}{2D}\right) \tag{8}$$

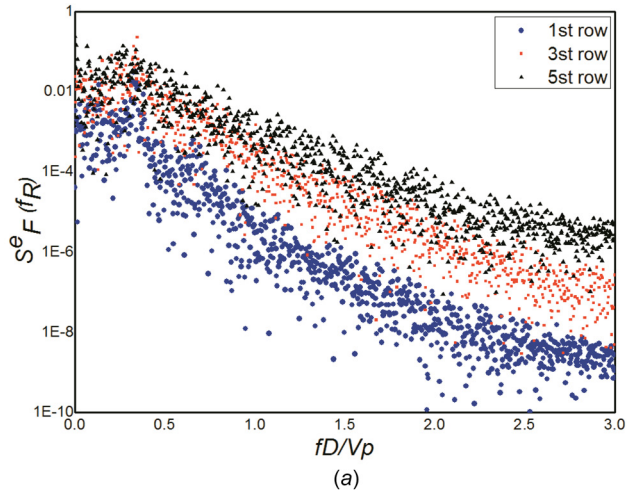

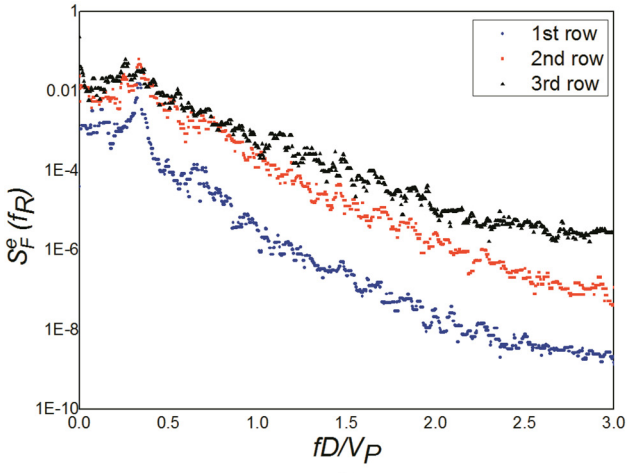

Fig. 9 Median filtering to lift force PSD

For ease of comparison, researchers in this field have used various methods of normalizing excitation force spectrum. Because the power spectral density (PSD) should be normalized using the dynamic pressure head, the dimensionless PSD, $S_F^e(f_R)$, can be expressed as follows:

$$S_F^e(f_R) = \frac{S_F(f)}{\left(\frac{1}{2\rho D V_P^2}\right)^2}\frac{V_P}{D} \tag{9}$$

where V_P is the gap velocity and f_R is the reduced frequency. Equation is general and applicable to tube arrays in cross-flow. However, the approach is derived with many simplifying assumptions, and the most important ones are the following: the turbulence forcing function is homogeneous, isotropic, and stationary [17].

The noise deviation of the original signal of PSD is obviously great, which has a great deal of interference on the analysis of data characteristics. $S_F^e(f_R)$ needs grasp the main characteristics of the original signal with median filtering [23,24]. Figure 9 shows the PSD of lift force before and after median filtering for tube 1, tube 3, and tube 5 at Re $= 2.29 \times 10^4$. The main characteristics of the random force can be preserved by median filtering, and the law is becoming much more intuitive.

Figure 10 shows the processed normalized PSD with median filtering versus the reduced frequency. $S_F^e(f_R)$ of fluid forces is nearly same when Re is from 1.79×10^4 to 5.38×10^4. The result

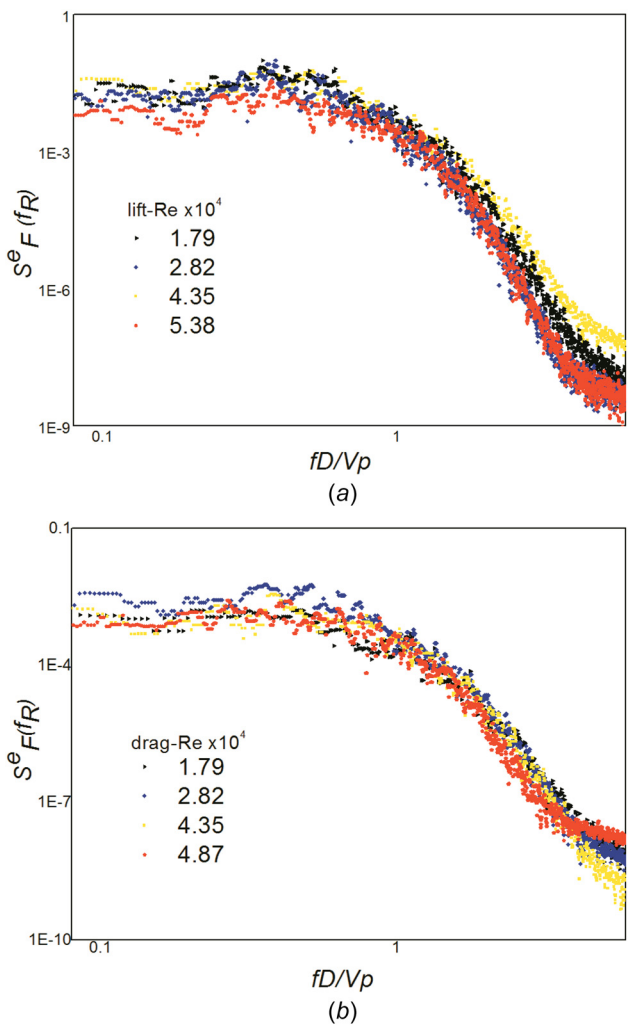

Fig. 10 Processed normalized PSD with median filtering

is consistent with Au-Yang et al. [22,25] and Taylor et al. [26]. The data are normalized and put on a common semilog plot. It shows that the nonconstant $S_F^e(f_R)$ between $f_R = 0.01$ and $f_R = 1$ is similar to a unimodal quasi-period pattern in low-frequency area. Meanwhile, a definite power low decaying trend between $f_R = 1$ and $f_R = 6$ is spotted with increasing f_R in high-frequency area. It is difficult to fit $S_F^e(f_R)$ through the entire range with a single equation. Mulcahy [27] has previously presented dimensionless data using equation as bounding spectra. The empirical equations can envelop the measured spectra. In the same manner, a simple fit to the data obtained in this study has been found for the wide band random component of the spectra.

Considering the existence of quasi-period features of lift force PSD, a bounded noise function model is applied to fit PSD of lift force in low-frequency area. The bounded noise is a harmonic function with a constant amplitude and random frequency [28]. Its spectral shape can be made to fit a target spectrum, such as the von Karman spectra of wind turbulence, by adjusting it parameters. Therefore, it can be a reasonable model for the random excitation or response in engineering systems. This model has been used for a long time in electrical engineering, but it is only recently used in hydromechanics and structural engineering [29,30]. The mathematical expression for the noise is

$$\xi(t) = \mu \sin(\Omega t + \psi) \tag{10}$$

$$\psi = \sigma B(t) + \chi \tag{11}$$

where $\xi(t)$ is a stationary random process in wide sense with zero mean; μ is the amplitude of bounded noise; Ω is the averaged circular frequency of bounded noise; σ is the constant representing intensity of random frequency; and χ is random variable uniformly distributed in $[0, 2\pi]$. Its covariance function is

$$c(\tau) = \frac{\mu^2}{2}\exp\left(-\frac{\sigma^2\tau}{2}\right)\cos(\Omega\tau) \tag{12}$$

And the variance of the noise is

$$c(0) = \frac{\mu^2}{2} \tag{13}$$

Its spectral density [31] is

$$S_\xi(f_R) = \frac{(\mu\sigma)^2}{\pi}\left(\frac{1}{4(f_R-\Omega)^2+\sigma^4} + \frac{1}{4(f_R+\Omega)^2+\sigma^4}\right) \tag{14}$$

In general, the function models with two main forms are applied to fit PSD of lift force in high-frequency area. They are the exponential function model [32] ($y = ka^x$) and the power function model [33] ($y = kx^a$), both of which having their own theory foundation and use range. Based on the feature of the experiment data in the current study, the power function model is applied, by analogy with the spectrum index in Kolmogorov theory [34] in high-frequency area, between $f_R = 0.01$ and $f_R = 1$.

According to the experiment results and the bounding value for $S_F^e(f_R)$ suggested by Au-Yang et al. [22] and Pettigrew and Gorman [32,35], an approximate estimate bounding spectra of PSD can be expressed as

$$S_F^e(f_R) = \frac{(\mu\sigma)^2}{\pi}\left(\frac{1}{4(f_R-\Omega)^2+\sigma^4} + \frac{1}{4(f_R+\Omega)^2+\sigma^4}\right) \text{ for } 0.01 < f_R < 1$$

$$S_F^e(f_R) = k \times {f_R}^a \quad \text{for } 1 < f_R < 6 \tag{16}$$

In Fig. 11, the measured and predicted PSD are plotted for tube 1, 3, and 5 over a wide range of Reynolds number, Re, from

1.79×10^4 to 5.38×10^4. Also, included in the figure are the predictions of $S_F^e(f_R)$ in the low-frequency region suggested by Oengoüren and Ziada [33], Blevins [21], and Pettigrew and Gorman [32,35]. Their results can only correspond with part of trends in low-frequency area and miss the features of peak of PSD. These plots show an excellent agreement between the result of the measured data and the equation. Note that the features of the quasi-period forces are more distinct and more severe in upstream tubes, and the amplitudes of the maximum of PSD varied are larger than those in downstream. The chaotic extent of fluctuations increases, which means the fluctuation is sensitive to the tube position. Although the predictions of Gorman Pettigrew are basically consistent with the experimental results, it is not enough to describe the details of the characteristics of $S_F^e(f_R)$, especially the change of the peak shape.

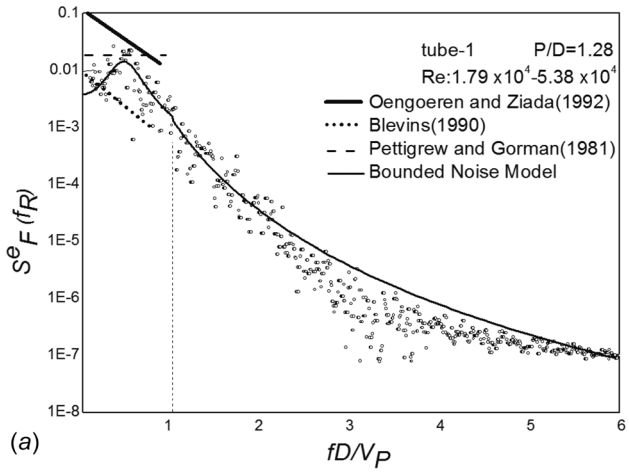

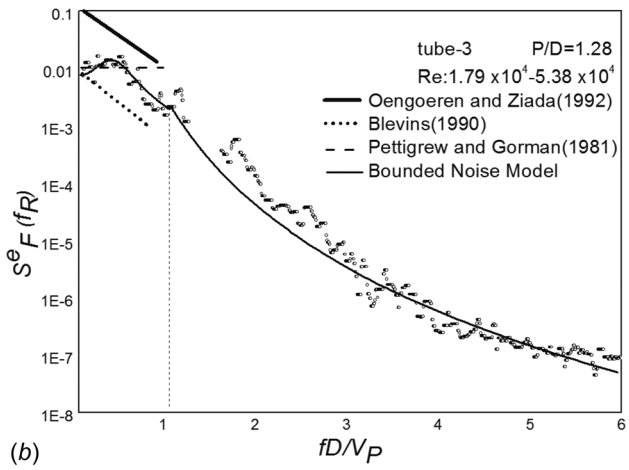

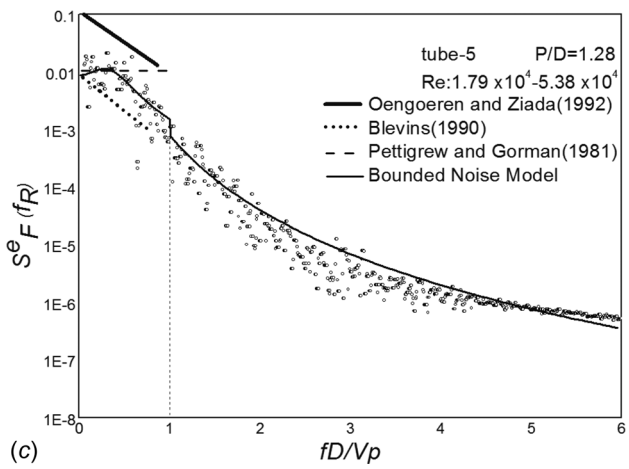

Fig. 11 Normalized lift force PSD for low-frequency area

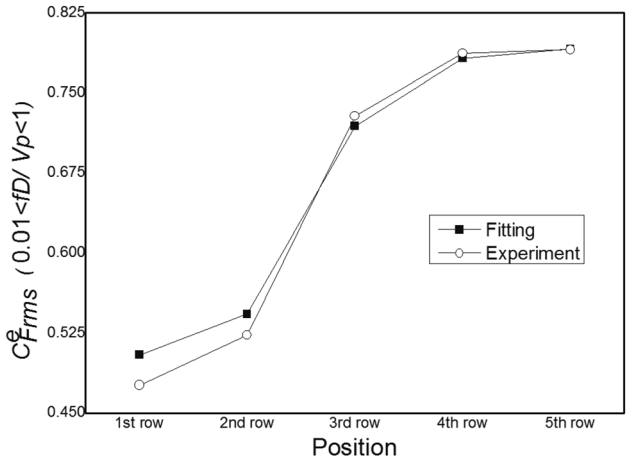

Fig. 12 Equivalent normalized excitation force coefficient for tube positions

The amplitude of bounded noise, μ, is equivalent to the amplitude of the effective fluid forces between $f_R = 0.01$ and $f_R = 1$ and can be obtained through the band-pass filter. Normalized excitation force coefficient, similar to C_l and C_d, is defined by the root-mean-square value of fluid forces in this range. Besides, the equivalent normalized excitation force coefficient, $C^e_{F_{\rm rms}}$, can be expressed as

$$C^e_{F_{\rm rms}} = \frac{F_{\rm rms}}{\frac{1}{2}\rho D L V_P^2}\left(\frac{V_P}{D}\right)^{\frac{1}{2}} \tag{17}$$

where $F_{\rm rms}$ is the root-mean-square value of fluid forces between $f_R = 0.01$ and $f_R = 1$. Figure 12 shows the experimental and fitting results about the equivalent normalized excitation force coefficient, $C^e_{F_{\rm rms}}$, from tube 1 to tube 5. It can be concluded that the model fits the actual situation well through the comparison of experimental data and the fitting parameters. With the enhancement of the disturbance, the overall value of the excitation force coefficient increases in low-frequency area. However, the excitation force coefficient grows at a snail's pace in the downstream tubes, which means the stability of the disturbance of fluid excitation forces with flow through the staggered array.

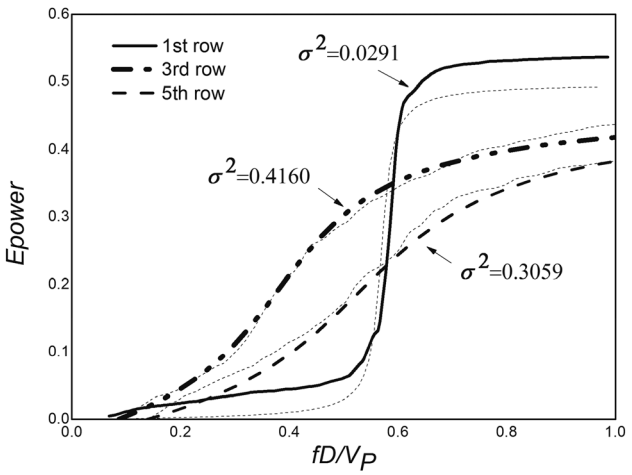

Fig. 13 Equivalent power of fluid forces for low-frequency area

The position and the bandwidth of the noise mainly depends on Ω and σ. Ω is determined by vortex shedding frequency, f_v, in the approximate equation, $\Omega = f_v D/V_P$. It is a narrow-band process when σ is small and it approaches to white noise when $\sigma \to \infty$. An integral equation about the equivalent power is selected to investigate the tendency of the PSD of fluid forces with the reduced frequency, excluding the impact of the amplitude of the effective fluid forces. The equivalent power [36], Epower, can be expressed as

$$\text{Epower} = \int_0^{f_R} \frac{S_F^e(f_R)}{\left(C_{F_{\text{rms}}}^e\right)^2} df_R$$

or

$$\int_0^{f_R} \frac{(\sigma)^2}{\pi} \left(\frac{1}{4(f_R - \Omega)^2 + \sigma^4} + \frac{1}{4(f_R + \Omega)^2 + \sigma^4} \right) df_R \tag{18}$$

Figure 13 shows the results of Epower versus the reduced frequency for tube 1, 3, and 5. Obviously, the distribution of PSD with frequency is decided by the number of Ω (tube $1 = 0.587$, tube $2 = 0.529$, and tube $3 = 0.38$) and σ. σ for downstream increases by roughly an order of magnitude means the increase of the noise bandwidth. The experimental results and the fitting parameters match very well. Compared with the results in downstream tubes, the shape of Epower for the first row is close to be perpendicular at St, while the variation of the shapes for tube 3 and tube 5 tends to be gentle and smooth. The power of the fluid forces for the first row centralizes in the frequency of vortex shedding, which leads to the sudden increase of Epower at St. Meanwhile, the magnitude for the first row is evidently greater than others between $f_R = 1$ and $f_R = 6$. The frequency position of the power concentration is dominated by the position of the tube. It is an interesting phenomenon.

More attention should be paid to the coupling effect of periodic and stochastic components in low-frequency area, which are, respectively, dependent upon $f_v D/V_P$ and σ. In addition, μ, which can characterize the amplitude of fluid forces, is taken into account in this model of $S_F^e(f_R)$ between $f_R = 0.01$ and $f_R = 1$. Meanwhile, bounded noise model can accurately represent the details of power spectral density, which fits well with the experimental data, especially considering about the coupling influence of periodic and stochastic components of fluid forces.

Figure 14 shows the results of normalized PSD of lift force in high-frequency area versus the reduced frequency from tube 1 to tube 5. The spectrum index is applied due to the analogy between the inertial subrange of the turbulent spectra and the high-frequency area in the current study. Though no obvious differences are obtained, the slight increase of the overall value of $S_F^e(f_R)$ has been gotten in the latter part of high-frequency area. And, the results are basically consistent with the suggested equation recommended by Oengoüren and Ziada [33].

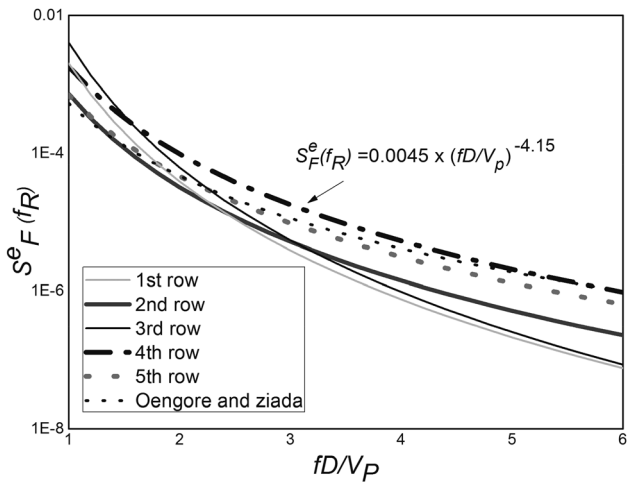

Fig. 14 Normalized lift force PSD for high-frequency area

For staggered and aligned configurations, it is not clear about the applicability of bounded noise model. In addition, it is very important for P/D which may have huge influence on these parameters of bounded noise. In fact, part of these parameters is related to C_l. Based on these, the approach for the unification and simplification of bounded noise could be proposed.

4 Conclusion

A bench-scale equipments were constructed to measure fluid excitation forces acting on cylinders in the normal triangular tube arrays ($P/D = 1.28$) with water cross-flow. Both of the periodic and stochastic forces, originated from vortex shedding and turbulence buffeting, were investigated with the characteristic parameters and mathematical model of fluid excitation forces.

In a tightly packed tube bundle, the influences of Reynolds numbers, from 1.79×10^4 to 5.38×10^4, on vortex shedding are much less conspicuous than the tube position. Meanwhile, the characteristic parameters of the fluctuating fluid forces become smaller or approximately constant for the interior tubes.

The periodic component originated from vortex shedding will gradually disappear with flow through the staggered array, while the coupling of the periodic and stochastic components of fluid excitation forces is emerging. It is difficult to make a precise determination of Strouhal number and fluid force coefficients in a tightly packed tube bundle.

The bounded noise and the spectrum index are applied for the characterization of PSD for fluid excitation forces through the entire frequency range. The quasi-periodic features of fluid excitation forces have been proven with the introduction of σ and μ. The results show that the bounded noise model can fit well with the experimental data, especially considering about the coupling influence of periodic and stochastic components of fluid forces.

Nomenclature

$B(t)$ = unit Wiener process
$c(\tau)$ = covariance function
$C_{F_{\text{rms}}}^e$ = nondimensional root mean of fluctuating force coefficient
D = tube diameter, m
Epower = nondimensional variance of fluctuating force coefficient
f_R = reduced frequency, Hz
f_v = Strouhal peak number, Hz
$F_{l\ \text{rms}}$ = the root mean of fluid forces, N
L = tube length, m
P = tube pitch, m
$S_F(f)$ = spectral density of fluctuating force per unit length ($0 < f < \infty$), $\text{N}^2\text{s/m}^2$
$S_F^e(f_R)$ = nondimensional spectral density
St = Strouhal number
μ = amplitude of bounded noise
$\xi(t)$ = bounded noise
σ = constant representing intensity of random frequency
χ = random variable uniformly distributed in $[0, 2\pi]$
Ω = averaged frequency of bounded noise, Hz

References

[1] Khushnood, S., Khan, Z. M., Malik, M. A., and Koreshi, Z. U., 2004, "A Review of Heat Exchanger Tube Bundle Vibrations in Two-Phase Cross-Flow," Nucl. Eng. Des., **230**(1–3), pp. 233–251.
[2] Song, M. T., Cao, D. Q., and Zhu, W. D., 2016, "Vortex-Induced Vibration of a Cable-Stayed Bridge," Shock Vib., **2016**(3), pp. 1–14.
[3] Xu, H. Q., Mallet, M., and Liszkai, T., 2014, "Turbulent Buffeting of Helical Coil Steam Generator Tubes," ASME Paper No. PVP2014-28868.

[4] Zhu, J., Wang, X. Q., and Xie, W. C., 2009, "Turbulence Effects on Fluidelastic Instability of a Cylinder in a Shear Flow," J. Sound Vib., **321**(3–5), pp. 680–703.
[5] Naudascher, E., and Rockwell, D., 2012, *Flow-Induced Vibrations: An Engineering Guide*, Dover Publishers, New York, Chap. 5.
[6] Blevins, R. D., 1974, "Fluid Elastic Whirling of a Tube Row," ASME J. Pressure Vessel Technol., **96**(4), pp. 263–267.
[7] Paidoussis, M. P., Price, S. J., and Mavriplis, D., 1985, "A Semipotential Flow Theory for the Dynamics of Cylinder Arrays in Cross Flow," ASME J. Fluids Eng., **107**(4), pp. 500–506.
[8] Chen, S. S., Zhu, S., and Jendrzejczyk, J. A., 1994, "Fluid Damping and Fluid Stiffness of a Tube Row in Crossflow," ASME J. Pressure Vessel Technol., **116**(4), pp. 370–383.
[9] Chen, S. S., 1987, "A General Theory for Dynamic Instability of Tube Arrays in Crossflow," J. Fluids Struct., **1**(1), pp. 35–53.
[10] Thorsen, M. J., Saevik, S., and Larsen, C. M., 2016, "Time Domain Simulation of Vortex-Induced Vibrations in Stationary and Oscillating Flows," J. Fluids Struct., **61**, pp. 1–19.
[11] Wang, X. Q., and Xie, W. C., 2006, "Force Evolution Model for Vortex-Induced Vibration of One Elastic Cylinder in Cross Flow," ASME Paper No. PVP2006-ICPVT-11-93875.
[12] Zhu, J., Wang, X. Q., and Xie, W. C., 2008, "Flow-Induced Instability Under Bounded Noise Excitation in Cross-Flow," J. Sound Vib., **312**(3), pp. 476–495.
[13] Price, S. J., Paidoussis, M. P., Macdonald, R., and Mark, B., 1989, "The Flow-Induced Response of a Single Cylinder in an Array of Rigid Cylinders," J. Fluids Struct., **3**(1), pp. 61–82.
[14] Pettigrew, M. J., and Ko, P. L., 1980, "A Comprehensive Approach to Avoid Vibration on Fretting in Shell and Tube Heat Exchangers," ASME PVP, **41**, pp. 1–18.
[15] Chen, S. S., and Jendrzejczyk, J. A., 1987, "Fluid Excitation Forces Acting on a Square Tube Array," ASME J. Fluids Eng., **109**(4), pp. 415–423.
[16] Heinecke, E. P., and Mohr, K. H., 1982, "Investigations on Fluid Borne Forces in Heat Exchangers With Tubes in Cross Flow," 3rd International Conference on Vibration in Nuclear Plant, Keswick, UK, Vol. 1, pp. 21–30.
[17] Weaver, D. S., Ziada, S., and Ay-Yang, M. K., 2000, "Flow-Induced Vibrations in Power and Process Plant Components-Progress and Prospects," ASME J. Pressure Vessel Technol., **122**(3), pp. 339–348.
[18] Païdoussis, M. P., 1983, "A Review of Flow-Induced Vibrations in Reactors and Reactor Components," Nucl. Eng. Des., **74**(1), pp. 31–60.
[19] Weaver, D. S., and Grover, L. K., 1978, "Cross-Flow Induced Vibrations in a Tube Bank—Turbulent Buffeting and Fluid Elastic Instability," J. Sound Vib., **59**(2), pp. 277–294.
[20] Zhang, C., Pettigrew, M. J., and Mureithi, N. W., 2009, "Further Study of Quasiperiodic Vibration Excitation Forces in Rotated Triangular Tube Bundles Subjected to Two-Phase Cross Flow," ASME J. Pressure Vessel Technol., **131**(3), p. 031303.
[21] Blevins, R. D., 1991, *Flow-Induced Vibration*, 2nd ed., Van Nostrand Reinhold, New York, Chap. 6.
[22] Au-Yang, M. K., Brenneman, B., and Raj, D., 1995, "Flow-Induced Vibration Test of an Advanced Water Reactor Model—Part 1-Turbulence Induced Forcing Function," Nucl. Eng. Des., **157**(1–2), pp. 93–109.
[23] Lathi, B. P., 2004, *Linear Systems and Signals*, Oxford University Press, Oxford, UK, Chap. 6.
[24] Wasylkiwskyj, W., 2013, *Signals and Transforms in Linear Systems Analysis*, Springer, New York, Chap. 7.
[25] Au-Yang, M. K., and Jordan, K. B., 1980, "Dynamic Pressure Inside a PWR—A Study Based on Laboratory and Field Test Data," Nucl. Eng. Des., **58**(1), pp. 113–125.
[26] Taylor, C. E., Pettigrew, M. J., and Axisa, F., 1988, "Experimental Determination of Single and Two-Phase Cross Flow-Induced Forces on Tube Rows," ASME J. Pressure Vessel Technol., **110**(1), pp. 22–28.
[27] Mulcahy, T. M., 1984, "Fluid Forces on a Rigid Cylinder in Turbulent CrossFlow," ASME Winter Annual Meeting, New Orleans, LA, Vol. 1, pp. 15–28.
[28] Lin, Y. K., and Cai, G. Q., 1995, *Probabilistic Structural Dynamics: Advanced Theory and Applications*, McGraw-Hill Professional Publishing, New York, Chap. 4.
[29] Dimentberg, M., 1992, "Stability and Subcritical Dynamics of Structures With Disordered Travelling Parametric Excitation," Probab. Eng. Mech., **7**(3), pp. 131–134.
[30] Lin, Y. K., Li, Q. C., and Su, T. C., 1993, "Application of a New Turbulence Model in Predicting Motion Stability of a Wind-Excited Long-Span Bridges," J. Wind Eng. Ind. Aerodyn., **49**(1–3), pp. 507–516.
[31] Frey, M., and Simiu, E., 1993, "Noise-Induced Chaos and Phase Space Flux," Phys. D: Nonlinear Phenom., **63**(3–4), pp. 321–340.
[32] Pettigrew, M. J., and Gorman, D. J., 1981, "Vibration of Heat Exchanger Tube Bundles in Liquid and Two-Phase Cross Flow," ASME PVP, **52**, pp. 89–110.
[33] Oengoüren, A., and Ziada, S., 1992, "Unsteady Fluid Force Acting on a Square Tube Bundle in Air Cross-Flow," 1992 International Symposium on Flow-Induced Vibration and Noise, Vol. 230, pp. 55–74.
[34] Pope, S. B., 2000, *Turbulent Flows*, Cambridge University Press, Cambridge, UK, Chap. 6.
[35] Pettigrew, M. J., 1981, "Flow-Induced Vibration Phenomena in Nuclear Power Station Components," Power Ind. Res., **1**(2), pp. 97–133.
[36] Nakamura, T., Fujita, K., Kawanshi, K., Yamaguchi, N., and Tsuge, A., 1995, "Study on the Vibrational Characteristics of a Tube Array Caused by Two-Phase Flow—Part II: Fluidelastic Vibration," J. Fluids Struct., **9**(5), pp. 539–562.